Origin of Luminescence in La 2 MoO 6 and La 2 Mo 2 O 9 and Their Bi-Doped Variants

Marie Colmont, Philippe Boutinaud, Camille Latouche, Florian Massuyeau, Marielle Huvé, Anastasiya Zadoya, Stéphane Jobic

Origin of luminescence in La_2MoO_6 and $La_2Mo_2O_9$ and their Bi doped variants

Marie Colmont,[1,*] Philippe Boutinaud,[2] Camille Latouche,[3] Florian Massuyeau,[3] Marielle Huvé,[1] Anastasiya Zadoya,[1] Stéphane Jobic[3]

[1] Université de Lille, CNRS, Centrale Lille, Université d'Artois, UMR 8181, Unité de Catalyse et Chimie du Solide, Lille, F-59000, France.

[2] Clermont Université Auvergne, SIGMA Clermont, Institut de Chimie de Clermont Ferrand, BP 10448, 63000 Clermont-Ferrand, France

[3] Université de Nantes, CNRS, Institut des Matériaux Jean Rouxel (IMN), F-44000 Nantes, France

Supporting Information Placeholder

ABSTRACT: In this paper, lanthanum molybdenum oxides (La_2MoO_6 and $La_2Mo_2O_9$) and their Bi-doped derivatives were investigated as potential rare-earth-free phosphors. An X-Ray diffraction analysis coupled with an EDX study confirmed the purity of the samples and the insertion of bismuth in 1 molar % amount. Kubelka-Munk transformed reflectance spectra clearly indicated that the insertion of Bi induces a shortening of the optical gap in La_2MoO_6 but has no impact on the one of $La_2Mo_2O_9$. Moreover, excitation and emission spectra evidenced a strong temperature quenching effect in all materials. Also the CIEx,y parameters at 77K are almost identical with or without Bi-doping for the two host lattices. Clearly, it was shown, combining experimental data, ab-initio calculations and empirical positioning of absorption bands that luminescence of Bi-doped La_2MoO_6 sample is mainly related to the host lattice itself and distortions induced by La/Bi substitution. The role of the Bi^{3+} dopant is indirect and the luminescence is mainly due to a Mo-O charge transfer rather than an on-site Bi^{3+} $^3P_{1,0} \rightarrow {}^1S_0$ transition. Concerning $La_2Mo_2O_9$, there is no effect following the insertion of Bi implying that the role of Bi is insignificant.

INTRODUCTION

Luminescent materials play a major role in our daily life. Applications are numerous and various going from indoor and outdoor lighting to smartphones, tablets, computer screens, medical devices, etc. Nowadays, many studies focus on LEDs (Light Emitting Diodes), and especially on white LEDs (WLEDs) to produce at low price a comfortable light, i.e. a warm light. Most commercialized WLEDs consist today of (In,Ga)N based blue LED chip combined with a yellow phosphor (typically $(Y,Gd)_3Al_5O_{12}$:Ce) blended with a red-emitting phosphor (typically Eu^{2+}-doped nitrides or sulfides) to reach the appropriate values of color rendering index for the domestic market.[1–3] However, the controversies associated with the possible harmfulness of the blue component, often too intense, that may trigger photochemical damages to the retina and the crystalline lens, are pushing the lighting industry to develop alternatives. Among them, technologies based on the use of a UV-LED chip such as (In,Ga)(P,N) in association with three phosphors (e.g. Y_2O_2S:Eu or SrS:Eu or $Sr_2Si_5N_8$:Eu, $SrGa_2S_4$:Eu and $BaMgAl_{10}O_{17}$:Eu for red, green and blue, respectively) look particularly attractive.[4] Whatever the low efficiency of red phosphors remains a bottleneck, which limits the launching of such devices on the market. In addition, all these light technologies require substantial amounts of rare earths (REs) as activators. This, owing to the ever-increasing demand of these chemical elements in the industry (consumed in magnets for wind power systems, metal alloys for batteries, etc) and their intrinsic high separation/purification cost (associated with a possible concomitant supply difficulties for geopolitical reasons), is creating some tension. In this context, RE-free luminescent materials are receiving a strong incentive. Here, the challenge consists in substituting REs in phosphors by other activators of higher availability. Hence, 3d transition metal (e.g. Cr^{3+}, Mn^{2+}, Mn^{4+}, Ni^{2+})[5] and ns^2 post-transition metal (e.g. Tl^+, Pb^{2+}, Bi^{3+}) cations[6] are scrutinized more in depth. Native defects in solids may also give rise to luminescence (e.g. oxygen vacancies[7]) while charge transfer transitions in d^0 transition metal ion containing inorganic materials (e.g. titanates, vanadates, niobates, tantalates, molybdates, tungstates) appear as an excellent alternative.[8,9] With this in mind, we have embarked on the elucidation of the luminescent properties of lanthanum molybdenum oxides (LMO) and their bismuth doped derivatives (LMO:Bi).

So far, LMO were mainly investigated for properties others than luminescence. Among all inorganic phases reported in the La_2O_3-MoO_3 binary system, $La_2Mo_2O_9$ remains without a doubt the most famous.[10] Namely, it was largely studied for its particular ionic conductivity properties at intermediate temperature (i.e. between 400 and 800°C),[11] giving applications in oxygen sensors, oxide electrolytes in solid oxide fuel cells (SOFC) or oxygen pumping devices.[12,13] Some of them show potentialities in catalysis. Hence, La_2MoO_6 was studied for its capacity to oxidize toluene selectively[14] while $La_2Mo_2O_9$ is highly selective for adsorption and separation of organic dyes.[15]

Only few articles are devoted to luminescence in lanthanum molybdates. So far, the emission was often associated with the presence of a RE dopant.[16,17] Investigations on $La_2Mo_2O_9$ and La_2MoO_6 doped with Bi^{3+} were carried out[18,19] but the intent was clearly to improve the ionic conductivity of the host lattice. Bi^{3+} is otherwise a very promising and non-toxic activator[20,21] that can be regarded as a relevant substitute for rare earths. Depending on the host lattice (HL), the luminescence of Bi^{3+} may cover a spectral range, spanning from UV to red in correspondence with intra- and/or extra- ionic transitions. Intra-ionic transitions have an inter-configurational character of the type $6s^16p^1$ ($^3P_{0,1,2}$,$^1P_1$) $\rightarrow 6s^2$ ($^1S_0$), where $^1S_0$ is the ground state of Bi^{3+} and $^3P_{0,1,2,}$ $^1P_1$ are the excited in order of increasing energy. Emission occurs typically from the $^3P_1$ state at ambient temperature and from the $^3P_0$ state at very low temperature. Extra-ionic transitions have charge transfer character that relate either to metal to metal charge transfer (MMCT) between the $Bi^{3+}(6s^2)$ dopant to a closed shell transition metal M^{n+} of the host lattice ($Bi^{3+}(6s^2)$ + $M^{n+}(d^0) \rightarrow Bi^{4+}(6s^1)$ + $M^{(n-1)+}$ (d^1)) or to an intervalence charge transfer (IVCT) between two nearby Bi^{3+} ions forming dimers (2 $Bi^{3+}(6s^2) \rightarrow Bi^{4+}(6s^1)$ + Bi^{2+} ($6s^26p^1$)). In our case, we used a nominal Bi^{3+} doping of 1 mol % in La_2MoO_6 and $La_2Mo_2O_9$ to minimize bismuth clustering.

EXPERIMENTAL SECTION

Synthesis of samples. Samples of $La_2Mo_2O_9$ and $La_{1.98}Bi_{0.02}Mo_2O_9$ (1), and La_2MoO_6 and $La_{1.98}Bi_{0.02}MoO_9$ (2) were prepared from stoichiometric amounts of $La(OH)_3$, MoO_3 and Bi_2O_3 previously decarbonated at 600°C in air. The reactants were thoroughly mixed and ground together, placed in an alumina crucible and fired at 600°C during 12h. Then, the samples were heated at 1000°C during 12h for (1) and 700°C during 12h for (2), respectively. The purity of all samples was further checked by powder X-Ray diffraction (PXRD). No impurity was detected at the XRD detection threshold.

X-ray powder diffraction analysis. X-ray powder diffraction analysis of each powder sample was performed at room temperature in the angular range of 2θ 5-80° with a scan step width of 0.02° using a D8 Advance Bruker AXS diffractometer in Bragg Brentano geometry equipped with a 1D Lynx-Eye detector. Rietveld refinements were performed using JANA 2006.[22]

Quantitative analyses were performed with a FEI TechnaiG2 20 microscope operating at 200 kV, fitted with an X-ray energy-dispersive spectroscopy (XEDS) microanalysis system. The atomic-ratios of the elements were determined by XEDS analyses, finding good agreement between analytical and nominal compositions in the crystallites.

Optical measurements. UV-Vis spectra were collected at room temperature using a Perkin Elmer Lambda 650 spectrophotometer in the 300–800 nm range. Before the measurement, the blank was measured using $BaSO_4$ (standard for 100% reflectance) in order to calibrate the device. Spectra were transformed into absorption one via the use of the Kubelka-Munk function $F(R)= (1-R)^2/2R$, where R is the diffuse reflectance.

Excitation and emission spectra were collected on a Horiba fluorolog 3 equipped with a 450W xenon lamp using a R13456 PMT from Hamamatsu for detection. Controlled temperature measurements were conducted by means of an optistat DNV Oxford cryostat. Excitation and emission wavelength for emission and excitation spectra were chosen to the maximum of signals at low temperature. CIE-1931 (2°) chromaticity coordinates of samples at 77K were calculated using the Osram Sylvania ColorCalculator (v7.63).

Computational details. All the computations were performed using the Vienna Ab-Initio Simulation Package (VASP).[23–25] Investigations were realized on the $La_{16}Mo_8O_{48}$ and $Bi_1La_{15}Mo_8O_{48}$ materials in order to retrieve a decent dilution of defects when Bi replaces La. Structure optimizations were performed enforcing a 12 × 12 × 4 k-mesh in both cases using a GGA +U (PBE) approach with U = 4.38 for Mo atoms and the cut-off energy was set to 500 eV. The optimized cell parameters of $La_{16}Mo_8O_{48}$ were kept unchanged to optimize the ion positions of the faulted cell ($Bi_1La_{15}Mo_8O_{48}$). On top of these relaxed geometries, Density of States (DOS) were simulated using a hybrid functional to ensure an accurate description of the electronic structure (HSE) of the investigated materials. These calculations were performed using a smaller k-mesh due to the high computational cost when one enforces such approach. All the post-treatments were done with the PyDEF suite.[26,27]

RESULTS AND DISCUSSION

Bi-insertion in the host matrix. La_2MoO_6, $La_{1.98}Bi_{0.02}MoO_6$, $La_2Mo_2O_9$ and $La_{1.98}Bi_{0.02}Mo_2O_9$ samples were prepared and characterized using X-ray diffraction techniques. No sub-product or extra phases were detected, and all collected patterns were perfectly refined via the Rietveld method based on the two mother structures (see Figure S1).

The successful insertion of bismuth was confirmed from EDS analyses of tiny single crystals. The quantification (Figure S2) agreed with the targeted compositions (1.98:0.019:0.79 and 1.98:0.014:1.68 measured La:Bi:Mo ratios for $La_{1.98}Bi_{0.02}MoO_6$ and $La_{1.98}Bi_{0.02}Mo_2O_9$, respectively) with Bi atoms expected to be incorporated at the La sites in view of respective Bi^{3+} and La^{3+} ionic radii (e.g. 1.31 Å vs. 1.30 Å for a coordination number of 8).

The X-ray diffraction analyses show that La_2MoO_6 and La_2MoO_6:Bi doped samples correspond to the γ-polymorph of La_2MoO_6 (SG: $I4_1/a$ c d Z with a= 5.8005(1) Å and c= 32.0459(3) Å for La_2MoO_6 and a= 5.8011(1)Å and c=

32.0563(4) Å for $La_{1.98}Bi_{0.02}MoO_6$). In this case, the unit cell parameters are slightly larger in presence of bismuth although the ionic radii are similar. This could reveal a stereoactivity of the $6s^2$ lone pair in this compound. The γ- crystal structure of this lanthanum molybdate (Figure 1a) consists of infinite double layers $^2/_\infty[La_4O_{12}]^{12-}$ 2D slabs built upon LaO_8 polyhedra sharing edges and separated from each other by isolated Mo^{6+} cations in tetrahedral coordination (see Figure 1a). There is only one independent crystallographic site both for La and Mo atoms.

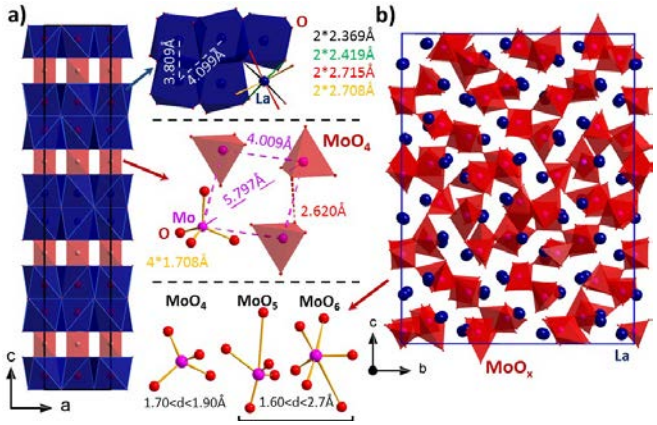

Figure 1. Crystal structures of a) La_2MoO_6 with the main interatomic distances within La_4O_{12} and MoO_4 units and of b) $La_2Mo_2O_9$ with the three MoO_x polyhedra.

The LaO_8 and MoO_4 environments are reproduced in Figure 1a with their La-O and Mo-O distances. Concerning $La_2Mo_2O_9$ and $La_{1.98}Bi_{0.02}Mo_2O_9$, both crystallize in the α-form of $La_2Mo_2O_9$ (SG $P2_1$, Z = 48, with a= 14.3581(3) Å, b= 21.4750(6) Å, c= 28.3927(6) Å and β= 90.27(2) ° for $La_2Mo_2O_9$, and a= 14.3276(2) Å, b= 21.4548(3) Å, c= 28.3941(4) Å and β= 90.37(1) ° for $La_{1.98}Bi_{0.02}Mo_2O_9$). The crystal structure is very complex with 312 distinct crystallographic sites, i.e. 48 for lanthanum and molybdenum, and 216 oxygen sites. The coordination of La^{3+} cations ranges from 6 to 12 (30 of the 48 La atoms are nine-coordinated) while Mo^{6+} cations exhibit three different oxygen environments as depicted in Figure 1b: 15 atoms are tetra-coordinated, 15 atoms are penta-coordinated, and 18 are hexa-coordinated. From our set of data, it was not possible to affect Bi to a preferential substituting La site.

The experimental optical band gaps of La_2MoO_6 and $La_2Mo_2O_9$ and their Bi doped variants were deduced from the examination of the Kubelka-Munk (KM) transformed diffuse reflectance spectra (Figure 2).[28] The absorption thresholds were calculated to 3.71 eV and 3.54 eV for La_2MoO_6 and $La_{1.98}Bi_{0.02}MoO_6$, and 3.09 eV and 3.06 eV for $La_2Mo_2O_9$ and $La_{1.98}Bi_{0.02}Mo_2O_9$, respectively. Naturally, absorption in La_2MoO_6 with only MoO_4 tetrahedra occurs at higher energy than in $La_2Mo_2O_9$ containing MoO_6 octahedra, the crystal field splitting of the d-block being larger in the latter case than in the former one. Although the band gaps decreases upon Bi-doping in La_2MoO_6, it is left unchanged in the case of $La_2Mo_2O_9$ (*vide infra*).

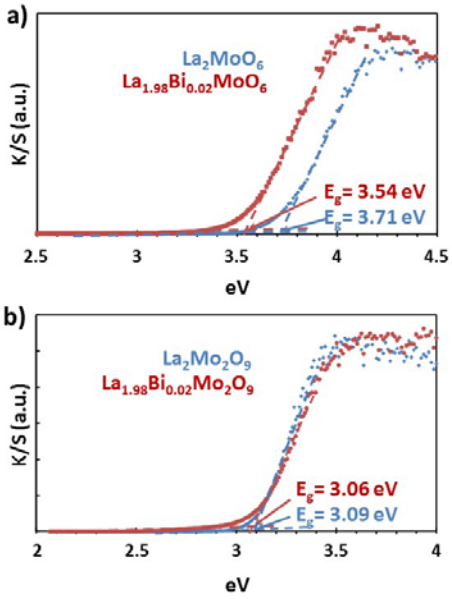

Figure 2. Kubelka–Munk transformed reflection spectra of a) La_2MoO_6 and $La_{1.98}Bi_{0.02}MoO_6$ and b) $La_2Mo_2O_9$, $La_{1.98}Bi_{0.02}Mo_2O_9$.

Excitation and emission spectra of La_2MoO_6, $La_2Mo_2O_9$ and their Bi-doped derivatives were collected from 77K to 300K (Figure 3). At low temperature, we observe a broad emission band peaking at ca. 700, 655, 655 and 640 nm (i.e. 1.77, 1.89, 1.89, 1.94 eV) for La_2MoO_6, $Bi_{0.02}La_{1.98}MoO_6$, $La_2Mo_2O_9$ and $Bi_{0.02}La_{1.98}Mo_2O_9$, respectively. The intensity of these bands drastically drops upon heating, indicating an efficient thermal quenching. This goes along with a high Stokes shift estimated at *ca*. 2.16, 1.92, 1.60, and 1.46 eV, respectively. The calculated CIEx,y parameters at 77 K are (0.59,0.40) for La_2MoO_6, (0.57,0.42) for $Bi_{0.02}La_{1.98}MoO_6$, (0.55,0.44) for $La_2Mo_2O_9$ and (0.55,0.43) for $Bi_{0.02}La_{1.98}Mo_2O_9$, i.e. values characteristic of saturated orange-red colors. As previously suggested by Wiegel and Blasse, [29] we ascribe the emission band observed for La_2MoO_6 and $La_2Mo_2O_9$ to a charge transfer, *i.e.* an electronic transfer from the bottom of the Mo-d block to the uppermost levels of the valence following $Mo\text{-}4d^1 + O\text{-}2p^5 \rightarrow Mo\text{-}4d^0 + O\text{-}2p^6$. Based on the evolution of the band gap going from La_2MoO_6 to $La_2Mo_2O_9$, an emission at shorter wavelength is expected in the former but the inverse is observed due to a larger Stoke shift. This advocates a higher lattice stiffness in $La_2Mo_2O_9$ than La_2MoO_6 in relation with a larger diversity of $[LaO_x]$ and $[MoO_x]$ polyhedra (*vide supra*) that agrees with a weaker ability of $[MoO_6]^{6-}$ octahedra than $[MoO_4]^{6-}$ tetrahedra to distort under light excitation. Let us notice that the position of the emission band is almost temperature independent in both compounds.

Doping with Bi does not alter the spectral features of $La_2Mo_2O_9$ significantly (identical CIEx,y parameters, *vide supra*) but modify substantially those of La_2MoO_6. First, the emission is blue-shifted by ca. 0.1eV, with no obvious change of its spectral position as temperature is varied. Second, the corresponding excitation spectrum, that consisted for the undoped material of an unique band undergoing a slight monotonic redshift of $2.7.10^{-3}$eV.K^{-1} as temperature was raised from 77K to 260K (see Figure S3 in Supplementary Information), now involves two largely overlapping contributions as evidenced by the spectral decompositions in Figure S4 (see Supplementary Information). The signal located to the high energy side vary from ca. 4.06 to 4.02 going from 77 to 260 K for instance with the same rate as virgin La_2MoO_6. We may suppose this signal originates from the same [MoO_4] tetrahedra, slightly blue-shifted due to Bi incorporation which softly disturbs the HL. The signal at lower energy vary from ca. 3.71 to 3.56 eV with a rate of 6.10^{-3} eV.K^{-1}, twice larger than in virgin La_2MoO_6. The corresponding Stokes shift, conversely, is substantially lower. At the lowest temperatures, this signal resembles the one reported initially by Wiegel and Blasse [29] for La_2MoO_6 (excitation at 3.76 eV, emission at 1.83 eV). Let us mention these authors also reported a $T_{1/2}^{4.2K}$ value (temperature at which the luminescence has lost 50 % of its 4.2 K intensity) of ca. 90 K in this material and a total quenching at 300 K, which matches satisfactorily with our observations for La_2MoO_6 and La_2MoO_6:Bi compounds ($T_{1/2}^{77K}$ of ca. 125 K determined for a reference temperature of 77 K). Whatever, to shed light on the luminescence properties of undoped and Bi doped La_2MoO_6, ab initio calculations were initiated to get insight on the energy location of 6s and 6p orbitals of Bi compared to 2p-O, 4d-Mo and 4d-La ones. Calculations were carried out on the $Bi_{0.125}La_{1.875}MoO_6$ composition only, i.e. $BiLa_{15}Mo_8O_{48}$ to simulate La_2MoO_6:1%Bi (calculations on $La_2Mo_2O_9$ and its Bi variant turned out to be very time consuming and did not converge).

Figure 4 sketches up the atomic contributions to the electronic structure. For the host cell, the computed band gap is calculated at 3.67 eV, in quite good agreement with experiment (3.71 eV). As aforementioned, the examination of the density of states (Figure S5) confirms that the valence band (VB) is built upon the "p" orbitals of oxygen while the empty "d" orbitals of Mo are the main characters of the conduction band (CB). Contribution of La-4d orbitals are repelled at higher energy. This result undoubtedly indicates that an oxygen to molybdenum charge transfer is at the origin of the observed absorption threshold (and emission of the host lattice). When one bismuth atom replaces one lanthanum atom, the electronic structure as a whole is barely affected.

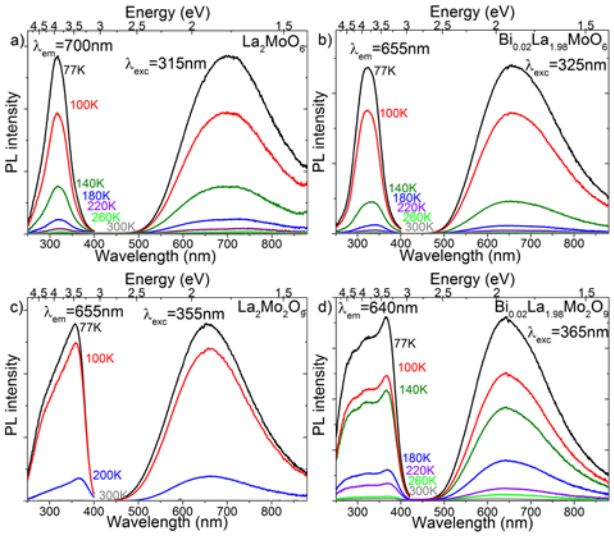

Figure 3. Temperature dependence of photoluminescence for a) La_2MoO_6, b) $Bi_{0.02}La_{1.98}MoO_6$, c) $La_2Mo_2O_9$ and d) $Bi_{0.02}La_{1.98}Mo_2O_9$.

Nevertheless, the diminution of the experimental band gap (3.71 vs. 3.54 eV) is accounted even though the difference is exaggerated in the calculation (3.22 vs. 3.54 eV). Namely, going from La_2MoO_6 to Bi doped La_2MoO_6, Bi-6s orbitals are interleaved at the top of the HL valence band, position in energy of the CB is not affected (or very slightly affected), and Bi-6p orbitals are located much higher than the bottom of the CB (Figure 4 a). The on-site $^1S_0 \rightarrow {}^3P_1$ and $^1S_0 \rightarrow {}^1P_1$ transitions (commonly labelled A and C bands, respectively) are anticipated to give rise to absorptions at ca. 3.48 and 4.52 eV. This is linked to the empirical equations $E_A(Bi^{3+},eV) = 2.97 + 6.2\ e^{-he/0.551}$ and $E_C(Bi^{3+},eV) = 3.23 + 10.92\ e^{-he/0.644}$ where he is a parameter depending on many factors such as the coordination number of Bi, its effective charge, the degree of covalence of the Bi-O bond, *etc* (he is calculated at 1.377 in La_2MoO_6 for Bi^{3+} at La^{3+} site based on a bond valence sum of 3.195 for La and 5.013 for Mo, respectively).[30-32] Noteworthy, we find that the predicted energy of the A transition in La_2MoO_6:Bi matches pretty well the experimental position (i.e. 3.56 eV) of the excitation threshold for T>180K (see Figure 3b and Figure S5) and gives credit to an attribution of this weak underlying band (or at least a part of it) to Bi. From these calculations, the $^3P_1$ and $^1P_1$ states would respectively be located at ca. 0.06 eV below and 0.98 eV above the CB bottom (Figure 4b).

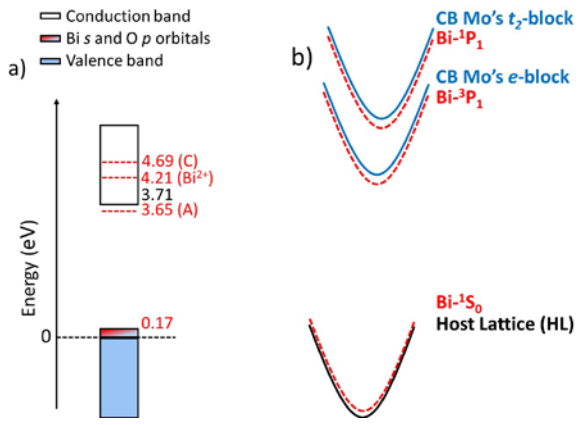

Figure 4. a) Schematic representation of the electronic structure of Bi doped La_2MoO_6 and b) schematic one coordinate configurational coordinate diagram of La_2MoO_6:Bi. The energy scale (*y* axis) in b) is relative and independent with respect to a).

Practically, based on the work of Boutinaud et al.,[31–34] it is also possible to determine the positioning in energy of the bismuth-molybdenum charge transfer based on the nowadays, well-established formulae MMCT(Bi^{3+}, eV) = 8.68 – 6.45 $\chi_4(Mo^{6+})/d_{corr}$ for Mo^{6+} cations in tetrahedral site, where $\chi_4(Mo^{6+})$ and d_{corr} stand for the optical electronegativity of Mo^{6+} cation for a 4-fold coordination and the shortest Bi-Mo distance in the understudied material, respectively. Using $\chi_4(Mo^{6+}) = 2.506$[35] and d_{corr}= 4.009 Å in the above equation, we estimate Bi^{3+} to Mo^{6+} MMCT at 4.6 ± 0.4 eV in La_2MoO_6:Bi, i.e. ca. 0.89 eV above the CB in an energy domain near the $^1P_1$ state. Typically, this MMCT would correspond to a transfer from the 6s orbital of Bi towards the t_2 (d_{xy}, d_{yz}, d_{xz}) orbitals of the Mo-4d block via the bridging oxygen atom instead of a direct straight ahead Bi-Mo charge transfer. However, the long Bi-Mo distance (~4 Å) with a Bi-O-Mo angle of ca. 120° seriously mortgages the eventuality of such an electronic transition. At the end, the so called Bi-Bi intervalence charge transfer for octa-coordinated Bi^{3+} dimers can also be estimated by the equation IVCT(Bi^{3+}, eV) = 11.43 –2/d_{corr} that is 4.21 eV for La_2MoO_6:Bi (d_{corr} = 3.814 Å).[34] Based on our previous conclusion, this implies that the $6p^1$ ground state of Bi^{2+} ($^2P_{1/2}$ state) would be *ca*. 0.5 eV above the conduction band, the IVCT being regarded at first sight as the energy separation between the Bi^{3+} and Bi^{2+} ground states (i.e. the energy needed to move one electron from one Bi^{3+} cation to another according to the 2 $Bi^{3+} \rightarrow Bi^{4+} + Bi^{2+}$ charge transfer).[36,37] Based on the position of this Bi^{2+} level, its participation to the absorption and the luminescence in La_2MoO_6:Bi is highly unlikely. Moreover, as luminescence of Bi^{2+} cations is associated to $^2S_{1/2} \rightarrow {}^2P_{1/2}$ and $^2P_{3/2} \rightarrow {}^2P_{1/2}$ transitions characterized by narrow emission bands, not observed at all in our prepared samples, this definitely rebuts the role of Bi^{2+} cations on the optical properties of La_2MoO_6:Bi. This conclusion could be prophesied, the presence of Bi^{2+} cations at the thermodynamic equilibrium being unlikely when syntheses are carried out in air without reducing post-treatment.

CONCLUSION.

Based on experiments, ab initio calculations and empirical positioning of absorption bands, we conclude that the low-temperature luminescence in Bi doped La_2MoO_6 images the spectroscopic behavior of oxygen-molybdenum charge transfers that undergo perturbations due to local structural distortions under the La/Bi substitution (stereoactivity of the $6s^2$ pair of Bi^{3+}) and electronic rearrangement of the charge density under the incorporation of Bi. We do not exclude a spectral contribution from Bi^{3+} but the close proximity of the 6s orbitals of Bi to the uppermost levels of the valence band and $^3P_1$ level to the CB bottom favors naturally thermal-assisted cross-over that readily leads to quenching, i.e. a (very) weak emission intensity, as temperature is raised.

In the case of $La_2Mo_2O_9$ and its Bi variant where absorption spectra are identical, we conclude that the role of Bi is not significant at all and the properties are majorly related to the host lattice.

▪ ASSOCIATED CONTENT

Supporting Information

The Supporting Information is available free of charge on the ACS Publications website xxxx at DOI: xxxx.

Materials preparation, characterization methods, computational details, Rietveld refinements and EDS analysis.

▪ AUTHOR INFORMATION

Corresponding Author

* E-mail: Marie.Colmont@centralelille.fr

Author Contributions

The manuscript was written through contributions by all authors.

Notes

The authors declare no competing financial interests.

▪ ACKNOWLEDGMENT

M.C. thank L. Burylo and N. Djellal for their technical assistance. The Chevreul Institute (FR 2638), the Ministère de l'Enseignement Supérieur et de la Recherche, the Région Hauts-de-France , the CNRS, and the FEDER are acknowledged for supporting and funding this work. The TEM facility in Lille (France) is supported by the Conseil Regional de la Région Hauts-de-France, and the European Regional Development Fund (ERDF).

C.L. thanks the Centre de Calculs Intensifs des Pays de la Loire for computational resources.

▪ REFERENCES

(1) A. Khare, S. Mishra, D. S. Kshatri, and S. Tiwari, « Optical Properties of Rare Earth Doped SrS Phosphor: A Review », *J. Electron. Mater.*, **2017**, *46*(2), 687-708.

(2) B. C. Cheng and Z. G. Wang, « Synthesis and Optical Properties of Europium-Doped ZnS: Long-Lasting Phosphorescence from Aligned Nanowires », *Adv. Funct. Mater.*, **2005**, *15*(11), 1883-1890.

(3) K. Van den Eeckhout, P. F. Smet, and D. Poelman, « Persistent Luminescence in Eu^{2+}-Doped Compounds: A Review », *Materials*, **2010**, *3*(4), 2536-2566,.

(4) J. K. Sheu, S.J. Chang, C.H. Kuo, Y.K. Su, L.W. Wu, Y.C. Lin, W.C. Lai, J.M. Tsai, G.C. Chi and R.K. Wu, « White-light emission from near UV InGaN-GaN LED chip precoated with blue/green/red phosphors », *IEEE Photonics Technol. Lett.*, **2003**, *15*(1), 18-20.

(5) M. G. Brik, S. J. Camardello, A. M. Srivastava, N. M. Avram, and A. Suchocki, « Spin-Forbidden Transitions in the Spectra of Transition Metal Ions and Nephelauxetic Effect », *ECS J. Solid State Sci. Technol.*, **2016**, 5, no 1, p. R3067-R3077.

(6) Z. Pei, A. van Dijken, A. Vink, and G. Blasse, « Luminescence of calcium bismuth vanadate ($CaBiVO_5$) », *J. Alloys Compd.*, **1994**, *204*(1-2), 243-246.

(7) Y. Wei, G. Xing, K. Liu, G. Li, P. Dang, S. Liang, M. Liu, Z. Cheng, D. Jin and J. Lin, « New strategy for designing orangish-red-emitting phosphor via oxygen-vacancy-induced electronic localization », *Light Sci. Appl.*, **2019**, *8*(1).

(8) L. K. Bharat, S.-K. Jeon, K. G. Krishna, and J. S. Yu, « Rare-earth free self-luminescent $Ca_2KZn_2(VO_4)_3$ phosphors for intense white light-emitting diodes », *Sci. Rep.*, **2017**, *7*(1).

(9) M. Colmont, S. Saitzek, A. Katelnikovas, H. Kabbour, J. Olchowka, and P. Roussel, « Host-sensitized luminescence properties of $KLa_5O_5(VO_4)_2:Eu^{3+}$ for solid-state lighting applications », *J. Mater. Chem. C*, **2016**, *4*(30), 7277-7285.

(10) P. Lacorre, F. Goutenoire, O. Bohnke, R. Retoux, and Y. Laligant, « Designing fast oxide-ion conductors based on $La_2Mo_2O_9$», *Nature*, **2000**, *404*(6780), 856-858.

(11) A. Tarancón, T. Norby, G. Dezanneau, A. Morata, F. Peiró, and J. R. Morante, « Conductivity Dependence on Oxygen Partial Pressure and Oxide-Ion Transport Numbers Determination for $La_2Mo_2O_9$», *Electrochem. Solid-State Lett.*, **2004**, *7*(10), A373.

(12) D. Marrero-López, J. Peña-Martínez, D. Pérez-Coll, and P. Núñez, « Effects of preparation method on the microstructure and transport properties of $La_2Mo_2O_9$ based materials », *J. Alloys Compd.*, **2006**, *422*(1-2), 249-257.

(13) C. Tealdi, G. Chiodelli, L. Malavasi, and G. Flor, « Effect of alkaline-doping on the properties of $La_2Mo_2O_9$ fast oxygen ion conductor», *J. Mater. Chem.*, **2004**, *14*(24), 3553.

(14) D. D. Agarwal, K. L. Madhok, and H. S. Goswami, « Selective oxidation of toluene over layered structures of Bi_2MoO_6 and La_2MoO_6», *React. Kinet. Catal. Lett.*, **1994**, *52*(1), 225-232.

(15) M. Sun, Y.Y. Ma, H. Tan, J. Yan and H.Y. Zang, «Lanthanum molybdenum oxide as a new platform for highly selective adsorption and fast separation of organic dyes», *RSC Adv.*, **2016**, *6*(93), 90010-90017.

(16) X. He, M. Guan, C. Zhang, T. Shang, N. Lian, and Q. Zhou, « Luminescence enhancement of Eu^{3+}-activated $La_2Mo_2O_9$ red-emitting phosphor through chemical substitution », *J. Mater. Res.*, **2011**, *26*(18), 2379-2383.

(17) a) F. Meng, X. Zhang, H. Li, and H. J. Seo, « Synthesis and spectral characteristics of $La_2MoO_6:Ln^{3+}$ (Ln=Eu, Sm, Dy, Pr, Tb) polycrystals », *J. Rare Earths*, **2012**, *30*(9), 866-870, b) U.H. Kaynar, S.C. Kaynar, Y. Alajlani, M. Ayvacikli, E. Karali, Y. Karabulut, S. Akca, T. Karali, N. Can, "Eu^{3+} and Dy^{3+} doped La_2MoO_6 and $La_2Mo_2O_9$ phosphors, Synthesis and luminescence properties", Mater. Res. Bul., **2020**, *123*, 110273.

(18) V. Voronkova, E. Kharitonova, and A. Krasilnikova, «Phase transitions and electrical conductivity of Bi-doped $La_2Mo_2O_9$ oxide ion conductors », *Phys. Status Solidi A*, **2009**, *206*(11), 2564-2568.

(19) P. S. Berdonosov, D.O. Charkin, K.S. Knight, K.E. Johnston, R.J. Goff, V.A. Dolgikh and P. Lightfoot, «Phase relations and crystal structures in the systems $(Bi,Ln)_2WO_6$ and $(Bi,Ln)_2MoO_6$ (Ln=lanthanide) », *J. Solid State Chem.*, **2006**, *179*(11), 3437-3444.

(20) H. C. Swart and R. E. Kroon, «(INVITED) Ultraviolet and visible luminescence from bismuth doped materials», *Opt. Mater. X*, **2019**, *2*, 10002.

(21) X. Liu, M. Xiao, L. Xu, Y. Miao and R. Ouyang, «Characteristics, Applications and Determination of Bismuth», *J. Nanosci. Nanotechnol.*, **2016**, *16*(7), 6679-6689.

(22) V. Petříček, M. Dušek, et L. Palatinus, « Crystallographic Computing System JANA2006: General features », *Z. Für Krist. - Cryst. Mater.*, vol. 229, nº 5, janv. 2014.

(23) G. Kresse et J. Furthmüller, « Efficiency of ab-initio total energy calculations for metals and semiconductors using a plane-wave basis set », *Comput. Mater. Sci.*, **1996**, *6*(1), 15-50.

(24) G. Kresse et J. Furthmüller, « Efficient iterative schemes for *ab initio* total-energy calculations using a plane-wave basis set », *Phys. Rev. B*, **1996**, *54*(16), 11169-11186.

(25) G. Kresse et D. Joubert, « From ultrasoft pseudopotentials to the projector augmented-wave method », *Phys. Rev. B*, **1999**, *59*(3), 1758-1775.

(26) A. Stoliaroff, S. Jobic, et C. Latouche, « PyDEF 2.0: An Easy to Use Post-treatment Software for Publishable Charts Featuring a Graphical User Interface », *J. Comput. Chem.*, **2018**, *39*(26), 2251-2261.

(27) E. Péan, J. Vidal, S. Jobic, et C. Latouche, « Presentation of the PyDEF post-treatment Python software to compute publishable charts for defect energy formation », *Chem. Phys. Lett.*, **2017**, *671*, 124-130.

(28) D. Driss, S. Cadars, P. Deniard, J.Y. Mevellec, B. Corraze, E. Janod and L. Cario, «Crystal structure and chemical bonding in the mixed anion compound BaSF», *Dalton Trans.*, **2017**, *46*(46), 16244-16250.

(29) M. Wiegel, G. Blasse, "The luminescence of octahedral and tetrahedral molybdates complexes", *J. Solid State Chem.*, **1992**, *99*, 388-394

(30) L. Wang, Q. Sun, Q. Liu, and J. Shi, «Investigation and application of quantitative relationship between sp energy levels of Bi^{3+} ion and host lattice», *J. Solid State Chem.*, **2012**, *191*, 142-146.

(31) M. Amer and P. Boutinaud, «On the character of the optical transitions in closed-shell transition metal oxides doped

with Bi^{3+}», *Phys. Chem. Chem. Phys.*, **2017**, 19(3), 2591-2596.

(32) M. Amer, «Using Semi-Empirical Models For Predicting The Luminescence –Structure Relationships in Near-UV Excited Phosphors Activated with Divalent Europium or Mercury-like Cations». University Clermont Auvergne, **2017**.

(33) P. Boutinaud, «Revisiting the Spectroscopy of the Bi^{3+} Ion in Oxide Compounds», *Inorg. Chem.*, **2013**, 52(10), 6028-6038.

(34) S. Mahlik, M. Amer, and P. Boutinaud, «Energy Level Structure of Bi^{3+} in Zircon and Scheelite Polymorphs of YVO_4», *J. Phys. Chem. C*, **2016**, *120*(15), 8261-8265.

(35) K. Li and D. Xue, «Estimation of Electronegativity Values of Elements in Different Valence States», *J. Phys. Chem. A*, **2006**, *110*(39), 11332-11337.

(36) P. Boutinaud, «On the luminescence of Bi^{3+} pairs in oxidic compounds», *J. Lumin.*, **2018**, *197*, 228-232.

(37) R. H. P. Awater and P. Dorenbos, «The Bi^{3+} 6s and 6p electron binding energies in relation to the chemical environment of inorganic compounds», *J. Lumin.*, **2017**, *184*, 221-231.

Entry for the Table of Contents

COMMUNICATION

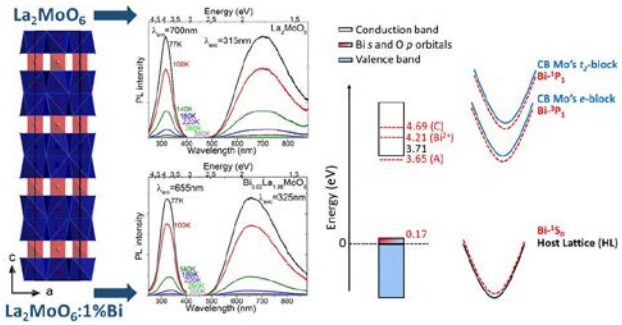

Marie Colmont,* Philippe Boutinaud, Camille Latouche, Florian Massuyeau, Marielle Huvé, Anastasiya Zadoya, Stéphane Jobic

Origin of luminescence in La_2MoO_6 and $La_2Mo_2O_9$ and their Bi doped variants.

La_2MoO_6 and $La_2Mo_2O_9$ and their Bi doped variants were fully investigated through analysis of optical properties correlated with ab-initio calculations and empirical positioning of absorption bands.